

# Cellular Compensatory Mechanisms in the CNS of Dysmyelinated Rats

Jacek M Kwiecien

Loss or absolute lack of myelin in the CNS results in remarkable compensation at the cellular level. In this study on the natural progression of neuropathology in the CNS in 2 related but distinct long-lived dysmyelinated rats, total lack of myelin was associated with remarkable glial cell proliferation and ineffective myelinating activity throughout life in Long Evans Bouncer (LE-bo) rats; conversely, in Long Evans Shaker (LES) rats, futile myelinating activity ceased when rats were advanced in age. Progressively severe astrogliosis separates individual axons from each other and coincides with widespread, abundant axonal sprouting throughout the life in both rat strains. Severely dysmyelinated Long Evans rats can serve as excellent models to elucidate the cellular and molecular mechanisms of neuroglial compensation to lack or loss of myelin in vivo and to study axonal plasticity in the adult demyelinated CNS.

**Abbreviations:** <sup>3</sup>H-TdR, [<sup>3</sup>H]-thymidine; LES, Long Evans Shaker; LE-bo, Long Evans Bouncer.

Compensatory cellular responses to loss of myelin in multiple sclerosis, experimental allergic encephalomyelitis or spinal cord injury, and both loss and absolute lack of myelin in dysmyelinated CNS are not well understood. Morphologic studies indicate that recent demyelinated lesions show proliferation of oligodendrocyte-type cells coinciding with repopulation of demyelinated areas and precocious remyelination.<sup>34,36,38</sup> Newly formed myelin sheaths are thin and may form shortened internodes that can be interspersed by demyelinated axonal segments.<sup>35</sup> Compensatory remyelination in human patients affected by multiple sclerosis<sup>26,34,41</sup> involves oligodendrocyte progenitor cells that populate the adult CNS and can be active in areas of demyelination.<sup>45,51,52</sup> However, remyelination is incomplete and fails altogether after recurrent bouts of demyelination.<sup>1</sup> Demyelinated plaques in sclerotic lesions can have surviving axons arranged in bundles which separated from each other by hypertrophied astrocyte processes.<sup>1</sup>

Cellular mechanisms of compensation in response to demyelination can be studied systematically and in detail in animal models of experimental allergic encephalomyelitis<sup>5,39</sup> or viral encephalitis, such as intracerebral inoculation of Theiler virus in CD1 mice.<sup>43</sup> Remyelination in areas of chronic demyelination requires increased mitotic activity, resulting in generation of astrocyte and oligodendrocyte progenitors and their migration into demyelinating areas with subsequent myelination and astrogliosis.<sup>8,37,40</sup> After immunoglobulin treatment of Theiler virus-inoculated SJL/J mice, their demyelinated lesions can have proliferation and maturation of oligodendrocyte progenitors followed by spontaneous remyelination.<sup>44</sup> Glial cell proliferation near lymphocytes and hypertrophied astrocytes suggested a beneficial role of at least some proinflammatory mechanisms in remyelination. Intracerebral in-

oculation of C57Bl/6N mice with mouse hepatitis virus produced demyelination followed by transient increase in proliferation of glial progenitors, which differentiated into oligodendrocytes and astrocytes with remyelination and astrogliosis.<sup>15</sup> Other experimental methods of demyelination, such as oral administration of cuprizone resulting in demyelination of cerebellar peduncles in CD1 mice<sup>25</sup> and intraspinal injection of ethidium bromide in rats,<sup>10</sup> have been used. Consistently demyelination was followed by increased mitotic activity with subsequent generation of astrocytes and oligodendrocytes and spontaneous remyelination and astrogliosis.<sup>10,25,27</sup>

Paracrine signaling involving oligodendrocytes and axons has been implicated in determination of the number of oligodendrocytes required to myelinate a population of axons in an area of CNS;<sup>3</sup> therefore, dysmyelinated rodent models can afford us insight into cellular mechanisms of compensation to hypomyelination.<sup>4,49</sup> The failure of the *jimpy* (*jp*) mouse, which carries a mutation in proteolipid protein,<sup>47</sup> to generate a normal amount of myelin results in severe hypomyelination due to oligodendrocyte dysfunction<sup>19,29</sup> and coincides with increased proliferation of cells of oligodendrocyte lineage that is balanced by increased oligodendrocyte death.<sup>2,9,18,47,53</sup> Vigorous proliferation of glial cell progenitors in the spinal cord and optic nerve of normal mice declines postpartum and is arrested or negligible by the third week of life.<sup>46</sup> In contrast, immature *jimpy* glial cells show even more robust proliferation in the neonatal life, as measured by intranuclear internalization of tritiated thymidine (<sup>3</sup>H]-TdR); this proliferation declines, as in glial cells of normal mice, but is still remarkable by the week 3.<sup>46</sup> In the spinal cord of *myelin-deficient* (*md*) rats, another severely dysmyelinated mutant strain with abnormal proteolipid protein, the proliferation of glial cells predominantly of oligodendrocyte lineage was increased as in *jimpy* cells, and inhibition of this proliferation was delayed until the third week postpartum.<sup>24</sup> Despite increased proliferation of oligodendrocytes during the postnatal period, the number of oligodendrocytes

Received: 06 Nov 2009. Revision requested: 12 Jan 2010. Accepted: 31 Jan 2010.  
Department of Pathology and Molecular Medicine and Department of Surgery, McMaster University, Hamilton, Ontario, Canada.  
Email: kwiecien@mcmaster.ca

markedly declined in relation to oligodendrocyte apoptosis in a longer-surviving substrain of *myelin-deficient* rats<sup>14</sup> suggesting the lack or insufficient proliferation of oligodendrocyte progenitors to counteract cell death. In the optic nerve of the Long Evans Shaker (LES) rat, a severely dysmyelinated but long-surviving rat with a mutation in myelin basic protein,<sup>30</sup> proliferation of glial cells is enhanced and their inhibition delayed, resulting in increased numbers of glial cells predominantly of oligodendrocyte morphology.<sup>22</sup> Inhibition of proliferation of oligodendrocyte progenitors was delayed in the spinal cord of *shiverer* (*shi*) mouse, another rat mutant in myelin basic protein, coinciding with a remarkable increase in oligodendrocyte numbers.<sup>6</sup> Although the molecular mechanisms regulating increased proliferation of oligodendrocyte progenitors and delayed inhibition of this proliferation in the postnatal period are unknown, a failure of myelination is considered to induce the proliferative response<sup>4</sup>

In severely dysmyelinated mutants such as the *shiverer* mouse and LES rat, oligodendrocytes develop pathology characterized by accumulation of a membranous material which forms vesicles limited by a pentalamellar membrane where at regular intervals 3 electron dense lines are separated by 2 electrolucent lines.<sup>13,22</sup> Analysis of electron micrographs of degenerating oligodendrocytes in cases of Pelizaeus–Merzbacher disease revealed that vesicles have limiting membrane with multiple dense lines regularly spaced at 5.8 nm.<sup>50</sup> Similar vesicles in degenerating oligodendrocytes have been observed in *jimpy* mice and LES and Long Evans Bouncer (LE-bo) rats, in which the dense lines in the vesicle walls are spaced at approximately 5-nm intervals.<sup>21,22</sup> Although the membranous material has not been analyzed chemically yet, its morphology including the regular periodicity of dense lines and formation of vesicles suggest a lipid-rich material whose hydrophobic properties induce it to form vesicles in the aqueous environment<sup>48</sup> of the mutated oligodendrocytes. In comparison, the periodicity of dense lines in the CNS myelin sheath averages 15 nm.<sup>23</sup>

Lack of myelin in the CNS coincides with astrogliosis, resulting in the enveloping of small bundles of naked axons by hypertrophied astrocyte processes, which effectively separates the axonal bundles from each other in *jimpy*<sup>19</sup> and *shiverer* mice<sup>19,33,42</sup> and LES<sup>22</sup> and old *taiep* rats (which progressively lose CNS myelin).<sup>28</sup> Review of electron micrographs in published literature revealed that small (less than 0.3  $\mu\text{m}$ ) structures containing neurotubules and neurofilaments, which are considered to be axonal sprouts, are common in dysmyelinated CNS in *jimpy*<sup>19</sup> and *shiverer*<sup>17,33</sup> mice and LES<sup>32</sup> and old *taiep*<sup>28</sup> rats. Although the precise mechanisms of

astrogliosis in which hypertrophied astrocyte processes separate bundles of naked axons are unknown, this reaction can be considered compensatory for lack of myelin and an attempt to isolate naked axons. Axonal sprouting, indicative of axonal plasticity in a severely dysmyelinated environment, has been demonstrated in the optic nerve of mature LES rats.<sup>32</sup> This observation supports the notion of inhibition of axonal plasticity and regeneration in presence of CNS myelin<sup>7,11</sup> but perhaps not in presence of hypertrophied astroglial processes; this finding also indicates the usefulness of dysmyelinated animals in *in vivo* studies of axonal regeneration relevant to spinal cord injury.

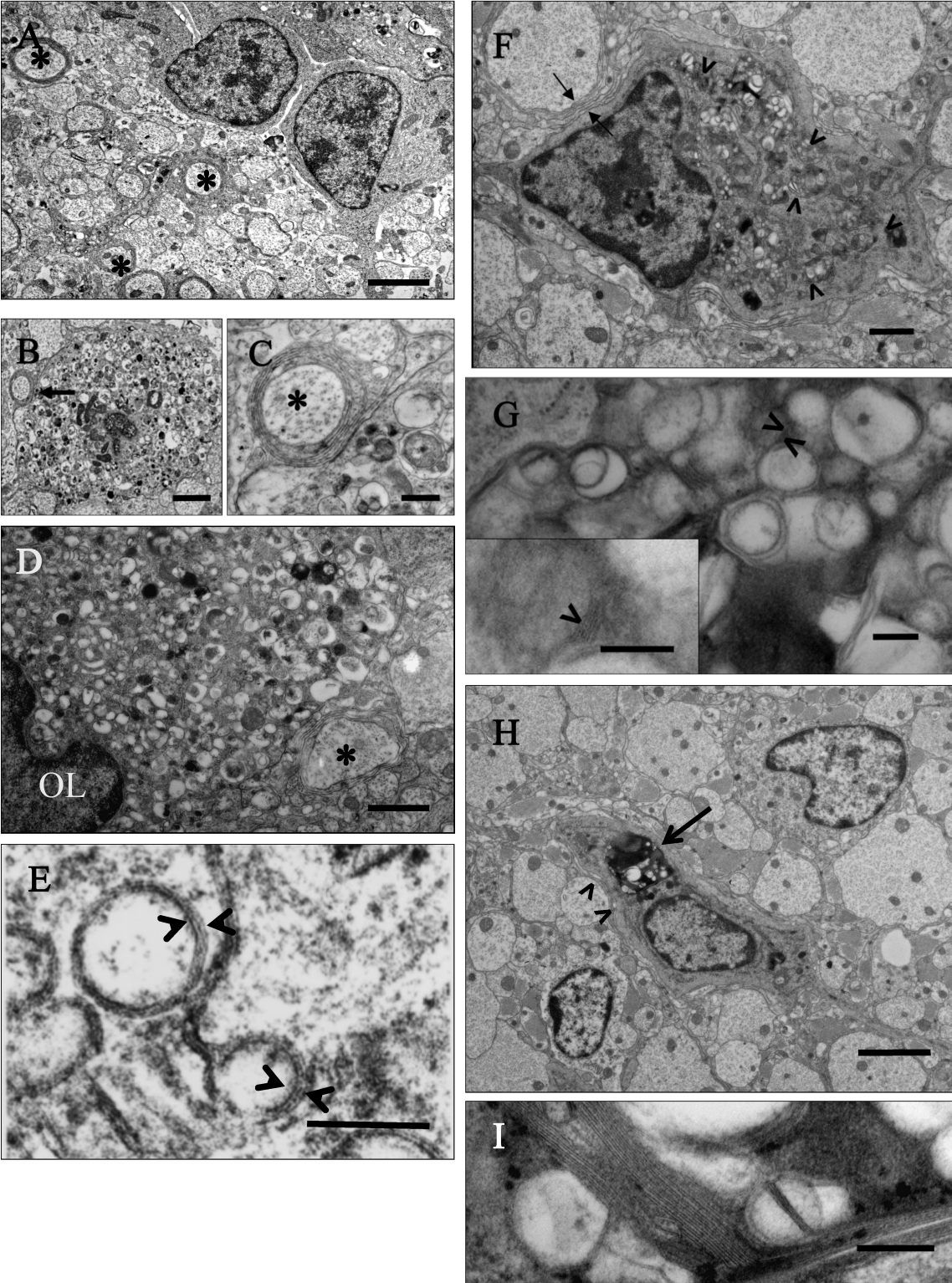
The present study was undertaken to analyze the natural progression of neuropathology in the CNS of 2 severely dysmyelinated long-lived mutant rat strains, LES and LE-bo, and to characterize the mechanisms of cellular response to lack of myelin.

## Materials and Methods

**Animals.** Two dysmyelinated rat phenotypes, LES and LE-bo, were studied along with control LE rats. The origins of LES and LE-bo rats are distinct. The LES mutant was first discovered in 1992 at McMaster University, Canada, in a breeding colony of Long Evans rats originally derived from a Charles River laboratories breeding stock (CrI:LE).<sup>12</sup> The LE-bo mutant rat was first discovered in 1990 at a Massachusetts Institute of Technology animal facility in a breeding colony of LE rats also originally derived from a CrI:LE stock.<sup>20</sup> Preliminary PCR analysis (not shown) indicated that both mutants are affected by the same mutation in the myelin basic protein gene.<sup>31</sup>

LES, control LE rats (phenotypically normal littermates of LES rats), and LE-bo rats were housed under a 12:12-h light:dark cycle in conventional rodent facility (Central Animal Facility, McMaster University) free of rodent viral infections, *Mycoplasma pulmonis*, and endoparasites and given rodent chow (Lab Diets, Purina Mills International, St Louis, MO) and tap water ad libitum. The rats were housed in shoebox-type cages on corncob bedding (Harlan Laboratories, Madison, WI). Husbandry and experimental procedures were approved by the Animal Research Ethics Board of McMaster University and conducted according to guidelines by the Canadian Council of Animal Care.<sup>31</sup> Dysmyelinated rats with spontaneous hindlimb paralysis and urinary bladder distended with hemorrhagic discharge<sup>21</sup> were considered to be at endpoint and were euthanized promptly in a CO<sub>2</sub> chamber. Both mutant strains of LE rat are prone to seizures and tonic-clonic convulsions,<sup>12</sup> sometimes resulting in hyperflexion of the spinal

**Figure 1.** Electron micrographs of progression of degeneration of oligodendrocytes in the spinal cord and optic nerve of LES rats 1 to 16 wk old. (A) Spinal cord of a 1-wk-old LES rat, in which 2 glial cells interpreted as immature oligodendrocytes are surrounded by dysmyelinated neuropil with few axons surrounded by thin sheaths (asterisks). Bar, 2  $\mu\text{m}$ . (B) Spinal cord of 1-wk-old LES rat. A degenerating cell is closely associated with a large adjacent axon (arrow) with a few uncompacted lamellae and numerous abnormal vesicular structures in the perikaryon. Bar, 2  $\mu\text{m}$ . (C) Detail of the thinly myelinated axon (asterisk) and degenerating changes in the perikaryon of panel B. Bar, 500 nm. (D) Optic nerve of 4-wk-old LES rat. A degenerating oligodendrocyte is closely adjacent to a large adjacent axon (asterisk). Its perikaryon is enlarged and contains small vesicular structures. Bar, 1  $\mu\text{m}$ . (E) Higher magnification of vesicular structures of panel D, which appear to be limited by a pentalamellar membrane (arrowheads) comprising 3 electron dense lines separated by 2 electrolucent lines with a regular periodicity. Bar, 100 nm. (F) Spinal cord of 8-wk-old LES rat. A degenerating cell forms uncompacted myelin membranes against a large adjacent axon (arrows), and its perikaryon is distended with multiple large aggregations of stacks of membranes or honeycombs (arrowheads). Bar, 1  $\mu\text{m}$ . (G) Higher magnification of panel F showing a fragment of a honeycomb with aggregated vesicular structures. In some areas there are stacks of membranes (arrowheads) that have a regular periodicity of approximately 5 nm between electron dense lines (arrowhead, inset). Bar, 200 nm (inset, 100 nm). (H) Spinal cord of 16-wk-old LES rat. An oligodendrocyte in the center of the image has numerous honeycombs in its perikaryon (arrow) with a few uncompacted myelin lamellae against large adjacent axons (arrowheads). Two adjacent cells appear to be immature oligodendrocytes. Wide astroglial processes separate individual axons from each other. Bar, 2  $\mu\text{m}$ . (I) Detail of a honeycomb with a stack of multiple membranes. Bar, 200 nm.



column and severe injury to midthoracic spinal cord<sup>20</sup> resulting in acute hindlimb paralysis and requiring immediate euthanasia. Only healthy male and female rats were used for collection of CNS tissues at 1, 2, 4, 8, 12, 16, 20, 24, 28, 32, 36, and 40 wk of age. Although natural longevity for LES rats was maximal at 93 wk of age ( $n = 1$ ), the additional oldest LES rat analyzed in this study was 69 wk for LES ( $n = 1$ ) and the oldest analyzed LE-bo rat was 45 wk old ( $n = 1$ ).

**Light and electron microscopy.** The rats were injected intraperitoneally with 2  $\mu$ Ci methyl[<sup>3</sup>H]-thymidine (<sup>3</sup>H-TdR, ICN, Irvine, CA) and then 90 min later deeply anesthetized with intraperitoneal injection of 65 mg/kg sodium pentobarbital (Ceva Sante Animale, Libourne, France). The thoracic cavity was opened, 0.2 mL heparin sodium (1000 U/mL, Pharmaceutical Partners of Canada, Richmond Hill, Ontario, Canada) was injected into the left ventricle by using a 30-gauge needle, and a 16-gauge needle attached to tubing primed with lactated Ringers solution (Baxter, Mississauga, Ontario, Canada) was inserted into the left ventricle. Flow of the lactated Ringers solution through the tubing was initiated, and a cut was made on the right auricle to create an outlet for blood. Within 4 to 6 min, the effluent from the right auricle became clear, at which point the lactated Ringers solution was replaced by a flow of Karnowski fixative containing 1.5% glutaraldehyde for 6 min and then with Karnowski fixative containing 5% glutaraldehyde which was the final fixative as described previously.<sup>21</sup> Brain, optic nerves, and spinal cord were dissected out and refrigerated at 4 °C in final Karnowski fixative. Midthoracic spinal cord and intracranial portions of the optic nerves were postfixed in osmium tetroxide, dehydrated in series of graded alcohols, and embedded in epoxy resin.<sup>21</sup> For light microscopy, semithin (1  $\mu$ m thick) sections of the optic nerve and spinal cord were mounted on glass slides and stained with toluidine blue. Silver-gray ultrathin sections from epoxy-embedded portions of the optic nerve and spinal cord were mounted on copper grids coated with polyvinyl formal, stained with uranyl acetate and lead citrate, and examined under transmission electron microscopy (1200EX Biosystem, Jeol, Montreal, Quebec, Canada).<sup>21</sup>

**Kinetics of glial cell proliferation.** Glial cells whose nuclei internalized <sup>3</sup>H-TdR were counted in 3 consecutive cross-sections 1 mm from the midthoracic spinal cord, and total glial cells were counted in the single cross-section of the intracranial optic nerve. Four LE control, LES, and LE-bo rats per age group (1 to 40 wk) were analyzed. In addition, one LES rat at the age of 69 wk and one LE-bo rat at 45 wk were examined.

For counts of glial cells, the intraorbital portion of the optic nerve was postfixed in osmium tetroxide, dehydrated in a series of graded alcohols, and embedded in epoxy resin, and 1- $\mu$ m thick cross-sections were mounted on glass slides and stained with toluidine blue. Meningeal cells (spindle in shape) and vascular cells (endothelial, vascular myocytes, and pericytes) were excluded so that only the glial cells in a single section per rat were counted under light microscopy (60 $\times$  dry objective; Eclipse 50i, Nikon, Toronto, Ontario, Canada). Counts from rats in each age and phenotypic group were averaged and the standard deviation calculated.

For counts of <sup>3</sup>H-TdR radiolabeled cells, 3 consecutive 1-mm-thick portions of midthoracic spinal cord of each rat were processed and embedded in epoxy resin; 1- $\mu$ m-thick cross-sections were mounted on glass slides and heat-sealed. The slides were immersed in NTB-II nuclear emulsion (Eastman-Kodak, Roch-

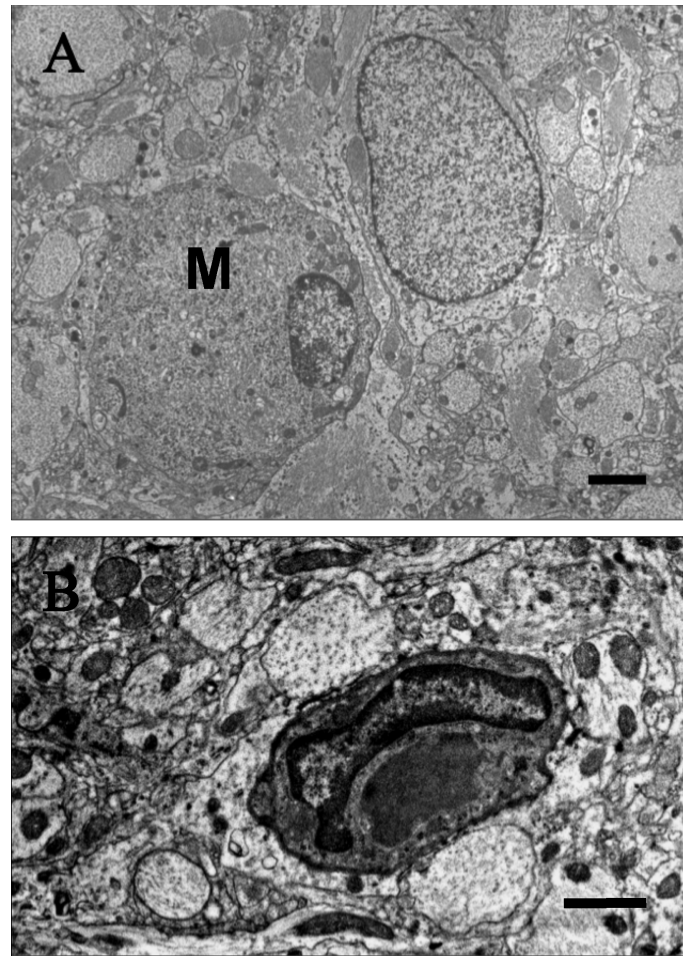


**Figure 2.** Microglial cells. (A) In this 24-wk-old LES rat, the round cell with a marginalized, elongated nucleus does not form myelin against adjacent axons and lacks vesicular structures and honeycombs in the perikaryon. This cell is considered to be a microglial cell (M) and is adjacent to an astrocyte. Bar, 4  $\mu$ m. (B) This microglial cell in a 12-wk-old LE-bo rat has a banana-shaped nucleus and a large, amorphous, moderately electron-dense inclusion in its cytoplasm. This cell does not form myelin against adjacent axons and lacks vesicular structures or honeycombs in the perikaryon. Bar, 2  $\mu$ m.

ester, NY) and exposed in the dark at 4 °C for 10 wk. These sections were developed and fixed according to the manufacturer's (Eastman-Kodak) instructions and then stained with toluidine blue and coverslipped. Cells with 4 or more coarse black grains over the nucleus were counted, and counts from 3 consecutive sections summarized for each rat. Counts from all rats in each age and phenotypic group were averaged and the standard deviation calculated. Glial cell counts in the optic nerves and the rate of glial cell proliferation and its differential distribution between the white and gray matter areas of the spinal cord were analyzed by using one-way factorial ANOVA (GraphPad Prism, version 2.01, GraphPad Software, La Jolla, CA).

## Results

**Neuropathology of oligodendrocyte degeneration in LES and LE-bo rats.** Consistent with previous studies on young LES<sup>22</sup> and LE-bo<sup>21</sup> rats, the LES and LE-bo rats analyzed in the current study

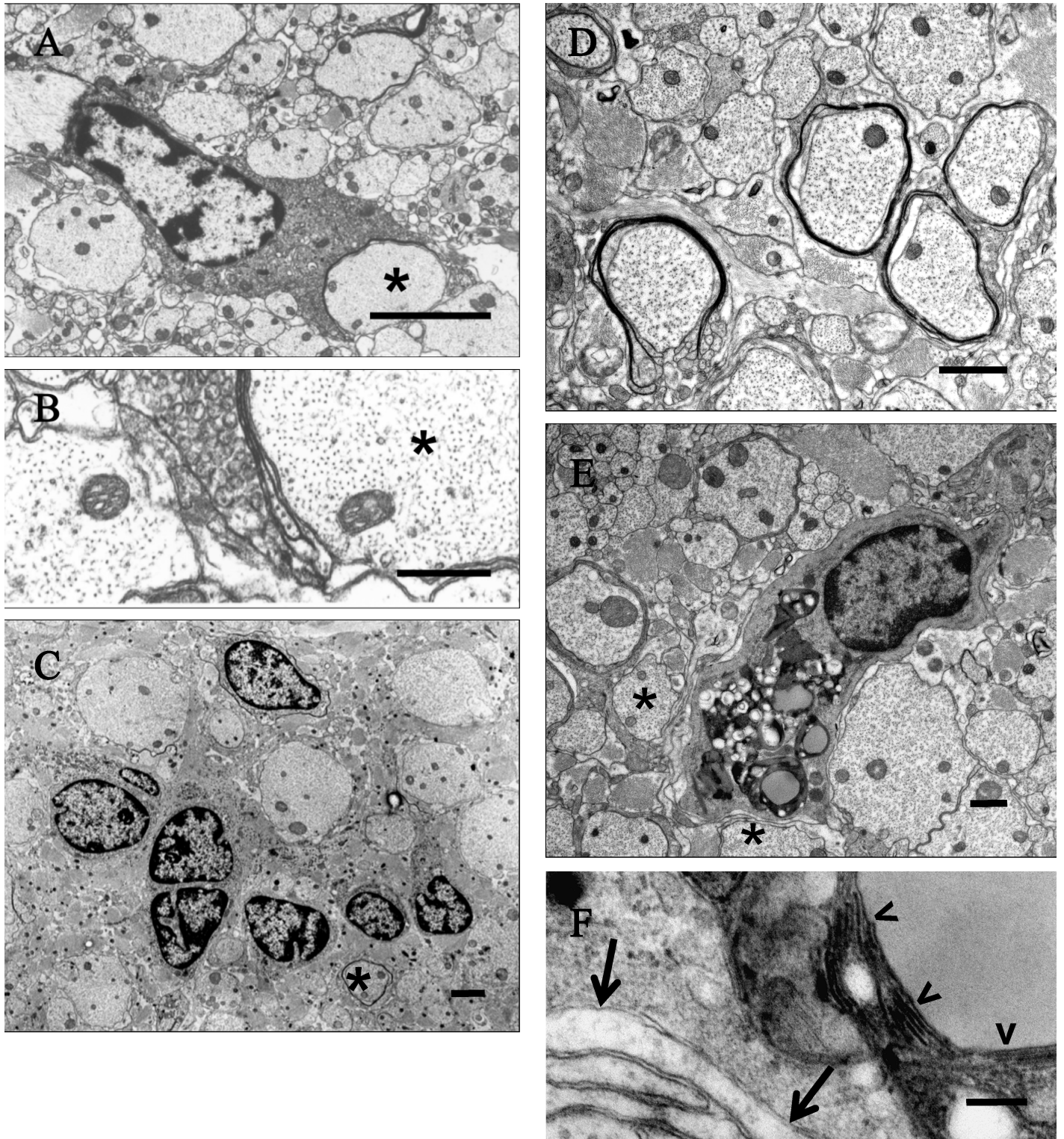


**Figure 3.** Ineffective myelinating activity by oligodendrocytes of the spinal cord and optic nerve of (A through C) adult LES and (D through F) LE-bo rats. (A) LES rat, 16 wk of age. An oligodendrocyte extends its perikaryon in attempt to myelinate a large adjacent axon (asterisk) with an incomplete myelin sheath. Bar, 2  $\mu$ m. (B) Detail of the incomplete myelin sheath in panel A. Bar, 500 nm. (C) LES rat, 69 wk. A cluster of glial cells interpreted as immature oligodendrocytes is surrounded by naked axons separated from each other by severe astrogliosis, with the exception of one axon that is surrounded by a single lamella (asterisk). Bar, 2  $\mu$ m. (D) LE-bo rat, 45 wk. Several axons have thin uncompact and sometimes incomplete sheaths. Bar, 1  $\mu$ m. (E) LE-bo rat, 45 wk. An oligodendrocyte forms a few incompact myelin lamellae against adjacent axons (asterisks), and its perikaryon is distended by honeycombs. Bar, 1  $\mu$ m. (F) Detail of the wall of a honeycomb encompassing stacks of multiple membranes (arrowheads) and of incompact myelin adjacent to the oligodendrocyte (arrows). Bar, 200 nm.

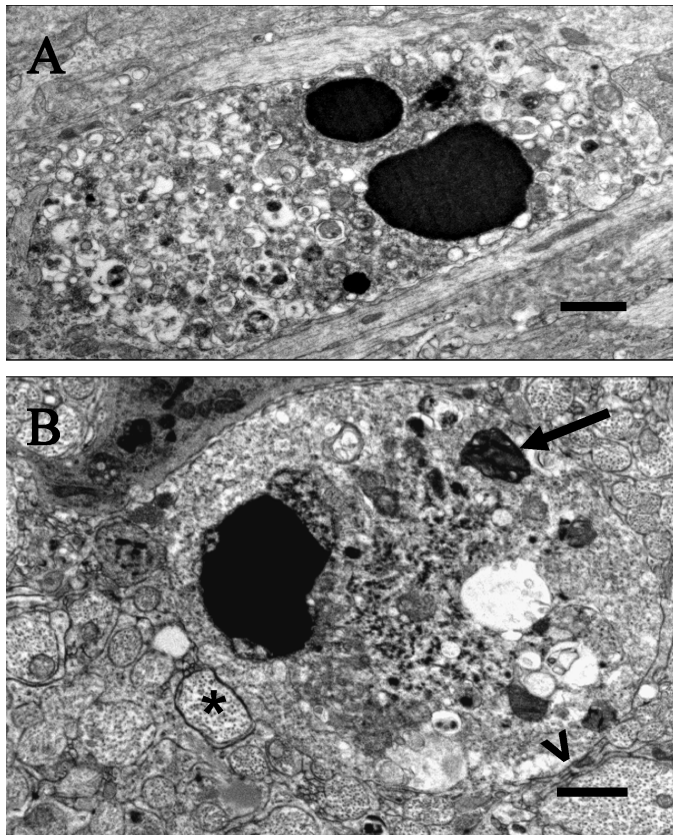


**Figure 4.** Glial cell death. (A) LES rat, 2 wk of age. An oligodendrocyte with a dense karyorrhectic nucleus and perikaryon distended with vesicular structures. Bar, 2  $\mu$ m. (B) LE-bo rat, 12 wk. A large oligodendrocyte with a pyknotic nucleus and perikaryon containing scattered vesicles and a large, dense, honeycomb structure. A large axon is separated from the cell membrane by few uncompact lamellae (open arrowhead); another adjacent axon has a thin uncompact sheath (asterisk). Bar, 1  $\mu$ m.

lacked normal, compacted myelin sheaths throughout their lives. Although scattered thin incompact myelin sheaths were readily apparent in LE-bo rats, at all examined ages, the numbers of such sheaths were markedly lower in 24- to 40-wk-old LES rats and were virtually absent in the single 69-wk-old LES rat available for analysis (data not shown).

In both LES and LE-bo rats, actively myelinating oligodendrocytes showed remarkable degenerative changes. Starting at 1 wk of age, this degeneration was characterized by loss of Golgi structures and apparent progressive accumulation of membranous material. This material appeared as vesicles of electrodense floccular material limited by a pentolamellar membrane with 3 dense lines separated by 2 lucent lines (Figure 1). In 4-wk-old LE-bo rats and 8-wk-old LES rats, vesicles in degenerating oligodendrocytes were replaced by larger, honeycomb-like stacks of membranous material; the spacing between multiple adjacent dense lines was approximately 5 nm, similar to the spacing between the dense lines in the pentolamellar membranes in the vesicles of oligodendrocytes in younger rats (Figure 1). Vesicle and 'honeycomb' morphology was essentially the same in LES and LE-bo rats. Degenerating oligodendrocytes often formed uncompact myelin lamellae between the cell membrane and adjacent axons (Figure 1) and were distinct from microglia, which were proportionally

rarer and had banana-shaped or oval nuclei with abundant cytoplasm rich in vesicles and small electrodense bodies and sometimes large inclusions (Figure 2). Microglia did not form myelin or accumulate membranous material in form of the vesicles or honeycombs characteristic of LES and LE-bo oligodendrocytes.

**Ineffective Myelinating Activity.** Ineffective myelinating activity has been reported to occur in the optic nerve and spinal cord of LES rats until 16 wk of age and in LE-bo rats until 14 wk.<sup>21,22</sup> In the present study, degenerating oligodendrocytes formed uncompact myelin sheaths until 16 to 20 wk of age in LES rats. After this age, this activity and the number of degenerating oligodendrocytes decreased. The proportion of glial cells thought to be immature oligodendrocytes increased in older LES rats; at the ages of 40 ( $n = 4$ ) and 69 wk ( $n = 1$ ) virtually all glial cells that were not viewed as astrocytes or microglial cells were interpreted to be immature oligodendrocytes. This increase in immature oligodendrocytes coincided with only very rare occurrence of thin myelin sheaths (Figure 3). In contrast, degenerating changes and accumulation of vesicles and honeycombs in oligodendrocytes persisted throughout life in LE-bo rats (Figure 3).

**Glial cell proliferation.** Low numbers of degenerating oligodendrocytes with dense, sometimes fragmented chromatin typical of pycnosis and karyorrhexis and increased numbers of cells with large perikaryon distended with numerous vesicles or honeycombs were found in the spinal cord and optic nerve of both strains of mutant rats throughout their lifespan (Figure 4). Both strains of mutant rats older than 16 wk had clusters of immature cells, including cells with large open nuclei and dispersed chromatin and perikarya containing intermediate filaments typical of astrocytes as well as cells with dark, often subcleaved nuclei with chromatin clumping on the nuclear periphery and perikarya with scattered microtubules typical of immature oligodendrocytes (Figure 5). The numbers of clusters of immature glial cells and the numbers of cells in those clusters both increased with age in both strains of mutant rats. Ependymal cells of the central canal in spinal cord sections lacked remarkable changes.

Counts of <sup>3</sup>H-TdR-positive cells histologically interpreted as glial cells in the spinal cord revealed that the abundant mitotic activity during the first week of life was rapidly, completely, and permanently inhibited in LE control rats before their second week. Glial cell mitotic activity was reduced but with considerable delay in both strains of dysmyelinated mutants and was never completely inhibited throughout their respective lifespans. Inhibition of glial cell mitosis reached its maximum at 8 wk in LES and 16 wk in LE-bo rats (Figure 6 A). LE-bo rats had higher ( $P < 0.005$ , one-way factorial ANOVA) numbers of <sup>3</sup>H-TdR-positive cells at 2 and 4 wk than did LES rats. Numbers of <sup>3</sup>H-TdR-positive glial cells increased after their maxima of inhibition in both mutant rat strains and reached shallow peaks at 16 to 20 wk in LES and at 28 wk in LE-bo rats, followed by declines in the numbers of positive cells.

Whereas oligodendrocytes with vesicles or honeycombs were abundant in the perikaryon of both strains of mutant rats, <sup>3</sup>H-TdR-positive cells had no such degenerative changes, indicating mitotic activity in immature, progenitor cells and not in maturing or degenerating cells. In particular, 1-wk-old control rats had 70% of <sup>3</sup>H-TdR-positive cells in their white matter, this proportion was even greater in the white matter areas in young, maturing, and old mutant rats (Table 1).

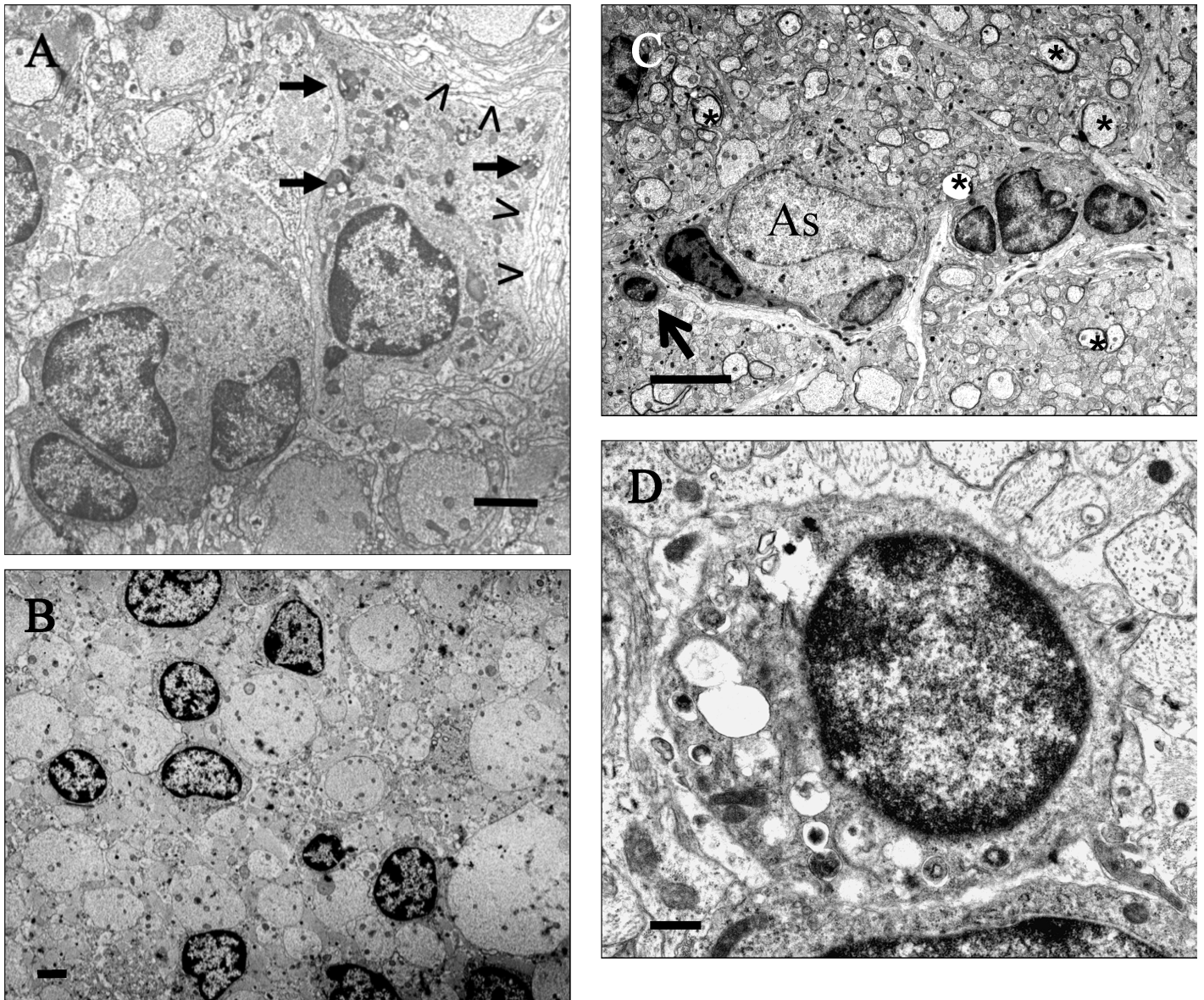


**Figure 5.** Glial cell plasticity in old LES and LE-bo rats. (A) LES rat, 24 wk of age. A mature oligodendrocyte forms incompact myelin lamellae against its membrane (open arrowheads) and contains numerous honeycombs scattered in the perikaryon (short arrows). Adjacent is a cluster of 4 immature glial cells. Bar, 2  $\mu$ m. (B) LES rat, 69 wk. Several immature glial cells are scattered among naked axons, which are separated from each other by astrogliosis. Bar, 4  $\mu$ m. (C) LE-bo rat, 45 wk. A cluster of immature glial cells of oligodendrocyte-type are adjacent to an astrocyte (As). In the surrounding area are scattered axons with thin myelin sheaths (asterisks). The arrow indicates an oligodendrocyte-type cell with multiple vesicles in the perikaryon, which are considered to be degenerative changes. Bar, 4  $\mu$ m. (D) Area indicated by the arrow in panel C. An oligodendrocyte-type cell with formation of vesicles in the perikaryon, which are considered to be degenerative changes. Bar, 500 nm.

Glial cell counts of the optic nerve included counts of oligodendrocytes, astrocytes, and microglial cells and excluded endothelial cells, vascular myocytes, pericytes, and meningeal cells.<sup>22</sup> The numbers of glial cells increased in all 3 rat phenotypes after the first week and reached a plateau of approximately 300 cells in the LE control rats at 4 wk and gradually, but not remarkably, decreased after 36 wk of age (Figure 6 B). In both strains of dysmyelinated rats, the numbers of glial cells continued to increase well into adulthood and reached a maximum and plateau of approximately 500 to 650 cells at 8 wk in LE-bo rats and approximately 700 cells at 16 wk of age in the LES rats. The number of glial cells in the optic nerve

of the single 69-wk-old LES rat available for study exceeded 1000 (Figure 6 A); this high count may be explained by the paucity of ultrastructural evidence of oligodendroglial degeneration at this old age (Figures 3 and 5). In contrast, oligodendrocytic degeneration persisted in abundance in old LE-bo rats including the oldest one (45 wk of age; Figure 3). These features perhaps contributed to the marked rate of death of persistently degenerating glial cells, which thus effectively prevented an increase in the total number of glial cells in old rats (Figure 6 B).

Pyknotic and karyorrhectic nuclei were present in the white matter of the spinal cord and optic nerve of both LES and LE-bo

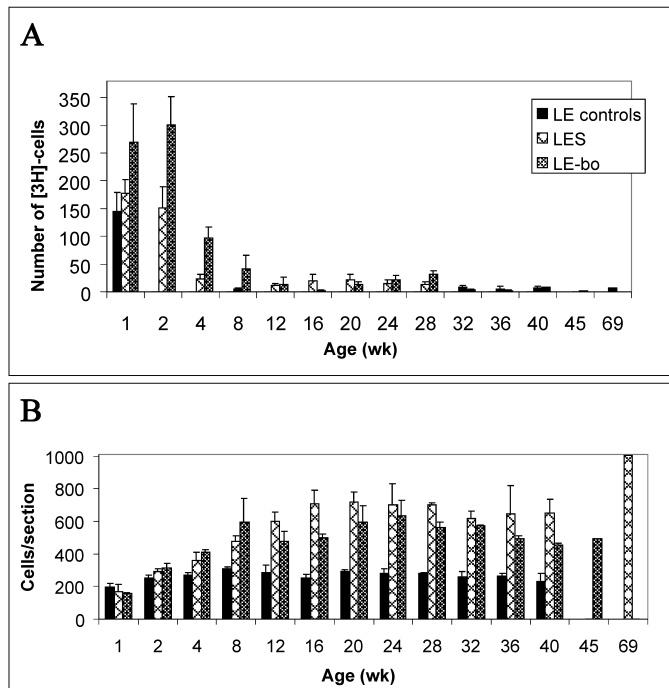


**Figure 6.** Glial cell proliferation in LES and LE-bo rats. (A) Glial cell proliferation in the spinal cord of LES, LE-bo, and LE-control rats (1 through 40 wk of age;  $n = 4$  per group) and single LES (69 wk) and LE-bo (45 wk) rats. For each rat, the numbers of [ $^3\text{H}$ ]-thymidine-positive glial cells were counted from 3 consecutive 1-mm-thick sections from the midthoracic spinal cord. Each column represents the mean  $\pm$  1 SD of the summaries of counts. The maximum inhibition of glial cell proliferation is at 8 wk for LES rats and at 16 wk for LE-bo rats. (B) Glial cells in a single section of the intracranial optic nerve collected from rats described in panel A. Each column represents the mean  $\pm$  1 SD of counts from each rat at the target age.

rats. However, cells with such changes were excluded from counts because they often contained dark blue-stained honeycombs difficult to distinguish from pycnotic or karyorrhectic nuclei (Figures 1 and 4). Also, honeycomb-containing oligodendrocytes with intact nuclei were difficult to differentiate from dying cells with nuclear changes.

A few ependymal cells were labeled in some rats of all 3 phenotypes but only at 1 and 2 wk of age, with the exception of a single ependymal cell that was labeled in an 8-wk-old LE-bo rat. Extraneural cells such as endothelial and meningeal cells were labeled in substantial numbers in all rat strains between ages 1 to 4 wk, after which labeling of such cells was rare.

**Axonal plasticity.** Morphologic abnormalities in axons of the optic nerve and spinal cord were not detected in the present study. Progressive severe astrogliosis in LES<sup>22</sup> and LE-bo<sup>21</sup> CNS coincided with separation of axons into small clusters by astrocytic processes in young rats; separations between individual axons increased with age (Figure 7). Starting at the age of 4 wk in both mutant strains, numerous clusters of small, round (less than 0.3  $\mu\text{m}$  in diameter) profiles containing neurotubules and neurofilaments were closely adjacent to large naked axons. These clusters were interpreted to be axonal sprouts<sup>32</sup> and were not separated from each other by astrogliosis. Often the clusters of sprouts lay between an axon and the cell membrane of an oligodendrocyte

or hypertrophied astrocyte (Figure 7), suggesting that neither of these glial-type cells inhibited this type of axonal plasticity. Axons with thin uncompacted myelin sheaths were not associated with sprouts in either LES or LE-bo rats.

## Discussion

Remarkable plasticity of glial cells including abundant mitotic activity, apparent differentiation of large proportion of new cells into oligodendrocytes, ineffective myelinating activity, and abundance of axonal sprouting despite severe widespread astrogliosis are hallmarks of neuropathology in dysmyelinated mutant LES and LE-bo rats throughout their long lifespan. Although CNS dysmyelination is more severe in both strains of LE mutants than in any other dysmyelinated animal model, LES rats can be maintained in good health as long as a normal laboratory rat for 93 wk and LE-bo for 45 wk. Both LES and LE-bo rats are fragile animals with rapid-frequency intention body tremor at young age and severe ataxia in older rats.<sup>12</sup> Severe tonic-clonic seizures coincide with spinal arching that sometimes results in hyperflexion of the spinal column and severe hemorrhagic-necrotizing damage to the spinal cord in midthoracic region.<sup>21</sup> This condition occurs unexpectedly, can affect as many as 50% of both LE mutant strains, results in hindlimb paralysis, and requires immediate euthanasia. Although sudden hindlimb paralysis in a large proportion of young LES and LE-bo rats makes them challenging models, rats older than 15 wk are considered resistant to this syndrome and are suitable for neurosurgical experiments requiring long-term postsurgical survival as long as 6 mo.<sup>21</sup>

In the severely dysmyelinated CNS, oligodendrocytes of both LE mutant rat strains infrequently attempted to form myelin sheaths around axons, typically of large diameter adjacent to the oligodendrocyte cell membrane. Formation of myelin sheaths coincided with accumulation of membranous material, with vesicles and then large honeycombs developing in degenerating oligodendrocytes in both mutant strains. A mechanistic explanation of this process should consider the interplay between naked axons that require myelin and inadequately responsive mutant oligodendrocytes. Molecular and genetic analysis of this compensatory cellular process likely would contribute to our understanding of the fundamental paracrine mechanisms of myelination and to effective treatment of loss of CNS myelin as occurs in multiple sclerosis, spinal cord injury, and brain injury, where persistent demyelination can cause permanent neurologic deficits. Ineffective myelinating activity persisted in LE-bo oligodendrocytes throughout their lifespan (as long as 45 wk). In contrast, whereas the process waned in older LES rats, in which oligodendrocytes with degenerative changes and located adjacent to axons with thin uncompacted sheath were virtually absent from the CNS at 40 and 69 wk of age. This observation may indicate differences in molecular interplay of oligodendrocytes and axons between LES and LE-bo rats. Furthermore, marked reduction in ineffective myelination activity in old LES rats coincided with virtual absence of oligodendrocytes with degenerative changes, prevalence of clusters of single immature glial cells, and a large increase in glial cell numbers in the optic nerve in the single rat examined at the age of 69 wk. The white matter in this rat contained many immature neuroglial cells, reminiscent of the white matter of normal neonatal rats. Although histologic delineation of gray matter is preserved in LES and LE-bo rats, lack of myelin makes their white matter appear grossly gray rather than shiny white, as in rats with

**Table 1.** Distribution of [<sup>3</sup>H]-thymidine-labeled cells in the spinal cord of LES, LE-bo, and LE control rats

Age (wk)	LES						LE-bo					
	White matter		Gray matter		P	White matter % mean	White matter		Gray matter		P	White matter % mean
	mean	1 SD	mean	1 SD			mean	1 SD	mean	1 SD		
1	143.5	17.7	35.2	6.4	0.000026	80.3	215.5	48.8	54.5	20.5	0.0500225	79.8
2	119.2	31.4	32.2	11.1	0.001967	78.7	237.2	39.8	64.5	11.9	0.0001642	78.6
4	20.2	8.0	3	1.4	0.005466	87.1	82	11.8	15	9.1	0.0014663	84.5
8	4.5	2.9	0	0	0.021000	100	37.5	22.0	3	4	0.0021504	92.6
12	11.5	2.1	0.7	0.5	0.000058	93.9	11.7	11.4	2	2.2	0.1457714	85.4
16	18.2	1.7	1.7	1.7	0.000009	91.2	1.7	0.9	0	0	0.0448489	100
20	20	6.5	1.7	2.4	0.001861	91.9	12.7	4.9	0	0	0.0020470	100
24	13.5	5.8	1.7	2.2	0.008921	88.5	20.5	7.1	1.2	1.3	0.0017484	94.2
28	12.2	5.9	1.2	1.0	0.010375	90.7	30.2	5.8	1	0.8	0.0000588	96.8
32	6.7	2.1	2	1.8	0.014521	77.1	3.3	1.1	0	0	0.0070000	100
36	5.5	3.7	0	0	0.002486	100	2	1	0	0	0.0260000	100
40	7	2.4	0.2	0.5	0.001449	96.5	6.7	2.1	1	1	0.0130000	87
LE control												
1	87	34.1	36.2	17.7	—	70.6						

Labeled cells were counted in 3 sections per rat, 4 rats per age group. Internalization of [<sup>3</sup>H]-thymidine was not observed in LE control rats after 1 wk of age. One-way factorial ANOVA was used to analyze differences in distribution of [<sup>3</sup>H]-thymidine-labeled cells between white and gray matter.

normal myelin. Other severely dysmyelinated mutants, including the *myelin-deficient* rat, have similar changes.<sup>14</sup>

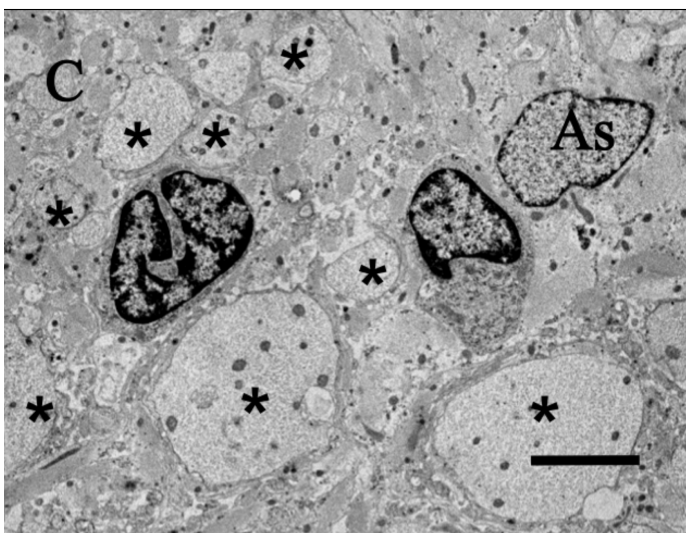
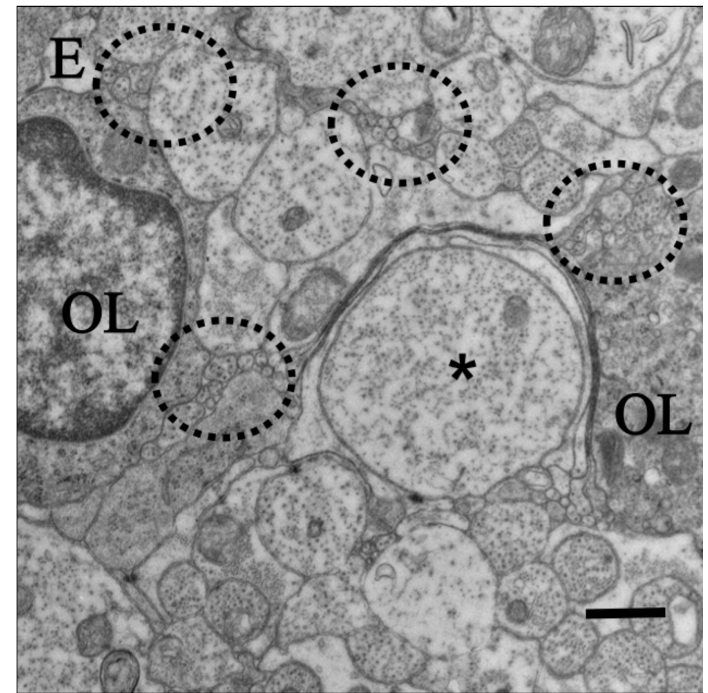
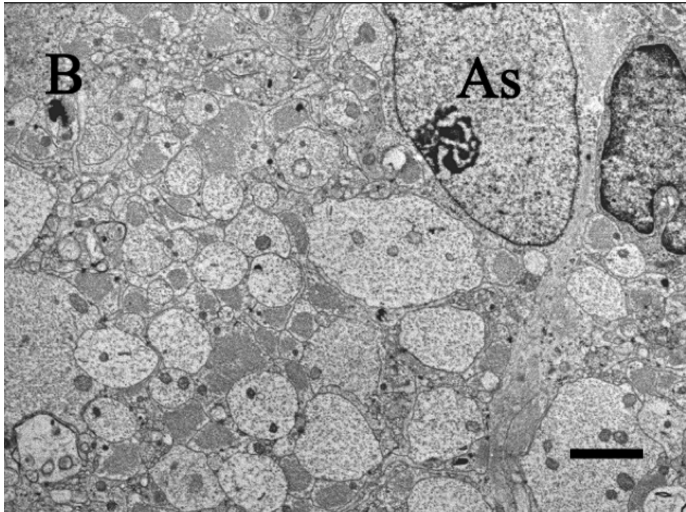
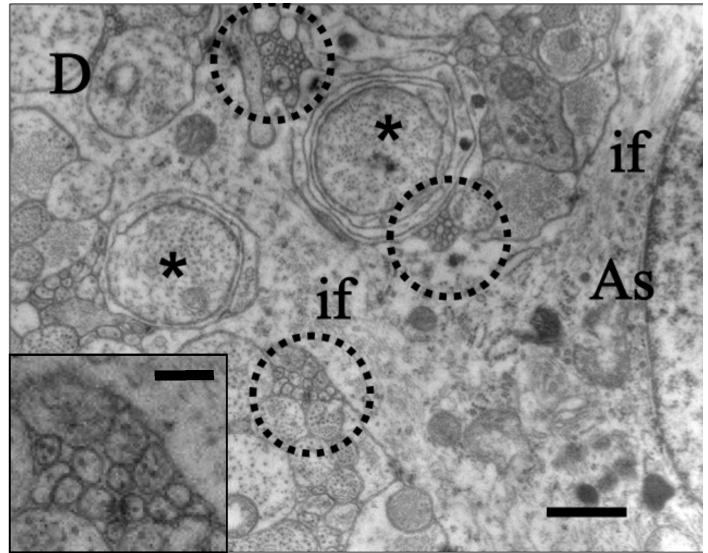
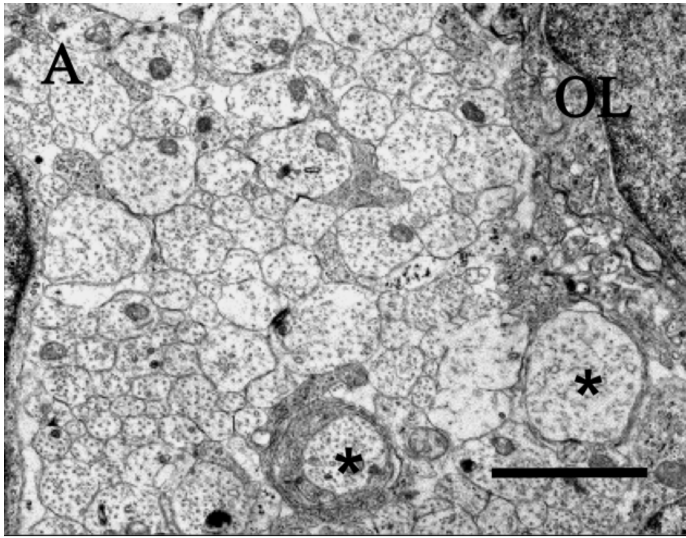
Proliferation of glial cells, another important cellular mechanism of compensation in the CNS, was analyzed by counting glial cells in the optic nerve and <sup>3</sup>H-TdR-labeled cells of glial morphology in the spinal cord. Examination of mitotic activity in glial cells in the spinal cord revealed no <sup>3</sup>H-TdR incorporation in control rats older than 1 wk. Two important issues are related to this observation. First, the glial cell proliferation was abundant in the CNS of normal neonatal rats, was rapidly, effectively, and permanently inhibited as analyzed with a single, 90 min pulse of <sup>3</sup>H-TdR in the present and previous studies.<sup>22,24,46</sup> Second, another study<sup>16</sup> demonstrated multiple glial cells incorporating bromodeoxyuridine, a thymidine analog, after daily injections of this indicator of DNA replication for 2 wk in adult rats. This finding demonstrated that low-level glial cell proliferation does occur in the CNS of normal adult rats and that most of this proliferation occurs in the white matter, suggesting scattered abundance of oligodendrocyte progenitors among mature oligodendrocytes.<sup>4</sup> The present study supports this notion. At the technical level, multiple intraperitoneal injections over a period of several days would be very difficult to achieve in fragile dysmyelinated rats such as the LES and LE-bo due to their propensity to seizure and to acute fatal hindlimb paralysis.<sup>21</sup>

Although inhibition of glial cell proliferation does occur in the spinal cord of both LES and LE-bo rats postneonally, this inhibition is delayed, gradual, incomplete, and comparable to the delayed and incomplete inhibition of glial cell proliferation in *jumpy*<sup>46</sup> and *shiverer*<sup>6</sup> and *myelin-deficient* rats.<sup>24</sup> Moreover, the differences in mitotic activity between LES and LE-bo rats from 2 to 8 wk of age are quite striking, allowing for a hypothesis that levels of molecular factors involved in inhibition of glial cell mitotic activity are considerably different between these strains during this time period. In adult LES rats, mitotic activity increases at 12 wk and peaks at 16 to 20 wk. The adult phase of glial cell proliferation in LE-bo rats has its onset at 20 wk and peaks at 28 wk. At

16 wk of age, the number of proliferating glial cells is 10× higher in LES than LE-bo rats. Whether molecular factors allowing the adult phase of glial cell proliferation in LES and LE-bo rats are related to diminishing inhibitory activity or increasing promitotic activity is unknown. Deciphering these important mechanisms will be possible when appropriate genomic studies are performed in these rats.

The distribution of dividing glial cells in both mutant strains of rats, primarily in the white matter of the spinal cord, is similar to the distribution of bromodeoxyuridine-positive glial cells in normal rats.<sup>16</sup> Glial cells in the LES and LE-bo rats were not characterized immunohistochemically in the present study, but the mitotic activity in the adult phase of proliferation may in fact involve glial cell progenitors. The present study provides 3 lines of evidence that support this notion. First, the greatest proportion of cells with mitotic activity (80% to 100%) occurred in the white matter area, away from the zone subjacent to the ependyma of the central canal. Second, mitotic activity within the ependymal lining (considered the source of neural stem cells) occurred only in 1- to 2-wk-old LES and LE-bo rats; among all the rats examined, only one 8-wk-old LE-bo rat showed any <sup>3</sup>H-TdR-positive labeling of a single ependymal cell. Third, <sup>3</sup>H-TdR-positive glial cells had no pathologic changes in the perikaryon of mature oligodendrocytes. Such changes were very characteristic and obvious on histologic examination of both LES and LE-bo rats.

Total numbers of glial cells in the optic nerve of control rats reached approximately 300 cells at 8 wk of age and then gradually and slowly decreased to approximately 240 by the age of 40 wk. In contrast, the numbers of glial cells in the optic nerve of the mutant strains increased at a greater rate and for a prolonged period of time, reaching approximately 700 at 16 wk of age in the LES rat. This finding is consistent with results from a previous similar study of the LES optic nerve.<sup>22</sup> In LES rats, this count remained essentially constant until 40 wk, perhaps because continuing mitotic activity of the adult phase of proliferation was balanced by cell death. However, at 69 wk the total number of



optic nerve glial cells increased markedly to more than 1000 in the one rat examined, coinciding with scant degeneration and ineffective myelinating activity in oligodendrocytes; these features may have contributed to the observed reduced rate of glial cell death. Glial cell death attributed to apoptosis is markedly elevated in postnatal *jimpy* mouse<sup>9,18,47</sup> and *myelin-deficient* rat<sup>24</sup> and is considered to cause a remarkable decline in oligodendrocyte numbers in aged *myelin-deficient* rats,<sup>14</sup> but the longevity of LES and LE-bo rats make these strains more attractive as *in vivo* models to study molecular mechanisms regulating glial cell proliferation and death in the adult CNS.

Previous studies on the progression of neuropathology in LES<sup>22</sup> and LE-bo<sup>21</sup> rats indicate diffuse astrogliosis and microgliosis with progressive severity. Histologic and ultrastructural examination of optic nerve and spinal cord tissues in the present and previous<sup>2,3,6,16</sup> studies indicate, however, that many of the cells generated during the observed abundant mitotic activity differentiate into oligodendrocytes.

The loss-of-function mutation in the myelin basic protein gene of LES,<sup>30</sup> and presumably LE-bo, rats correlated with metabolically active oligodendrocytes. Unsuccessful attempts at myelination coincided with ultrastructural pathology characterized by progressive accumulation of a membranous material in the perikaryon. The progression in the pathology of LES and LE-bo oligodendrocytes suggests that abundant metabolic activity designed to rapidly form vast quantities of myelin is not shut down at the end of neonatal stage, as in normally myelinating rats, but remains vigorous in both LES and LE-bo rats. Some metabolites, perhaps rich in lipids, apparently are not efficiently metabolized in mutant oligodendrocytes and progressively accumulate in the perikaryon as vesicular structures limited by pentalamellar membrane and then a honeycomb structures formed by polyhedral stacks of membranes with regular periodicity. The periodicity of 5 nm may suggest that the membranous material is rich in lipids, which are known to form asymmetric bilayers in an aqueous environment, resulting in formation of lipid vesicles.<sup>48</sup> The membranous material in degenerating LES and LE-bo oligodendrocytes should not be confused with myelin sheaths, which in the normal CNS have periodicity of 15 nm between adjacent electrodense lines.<sup>23</sup> The progressive accumulation of membranous material in form of vesicles often seemed to contribute to abnormal enlargement of perikaryon. The formation of honeycombs instead of vesicles in older rats can be interpreted as attempts by oligodendrocytes to conserve space in the perikaryon or to neutralize the presumably toxic effect of progressively accumulating abnormal membranous material.

Oligodendrocytes in other severely dysmyelinated subjects, including human patients with Pelizaeus–Merzbacher disease<sup>50</sup> and *shiverer*<sup>13</sup> and *jimpy* mice, also develop an accumulation of mem-

branous material that often forms vesicles limited by a membrane with regular periodicity in which adjacent electrodense lines are separated by a electrolucent line 5.0 to 5.8 nm in width. This accumulation of membranous material in oligodendrocytes in multiple dysmyelinated mutants and its consistent morphology of periodicity suggest its lipid nature and its strong relation to the inability of oligodendrocytes to form myelin sheaths and their ineffective myelinating activity.

Degenerating oligodendrocytes of LES and LE-bo rats often showed ineffective myelinating activity near adjacent axons, and the perikarya of these degenerating cells contained scattered microtubules and characteristic vesicles and honeycombs. The degenerating oligodendrocytes were distinct from microglia, which contained banana-shaped nuclei and never formed either myelin or honeycombs. The previous interpretation of abnormal cells with honeycombs as microglia<sup>54</sup> is therefore incorrect and has likely led to conclusions that need reevaluation. Appropriate recognition of indigenous LES glial cells, especially oligodendrocytes, is essential for the accurate interpretation of ultrastructural changes that occur in cell implantation and axonal regeneration experiments involving adult LES rats.<sup>20</sup>

LES and LE-bo rats show differences in the 1) kinetics of glial cell proliferation, 2) age at which ineffective myelinating activity declines, 3) age at which oligodendrocyte pathology progresses,<sup>21</sup> 4) body weight of adult animals,<sup>21</sup> and 5) date and location of strain origin.<sup>12,21</sup> These differences indicate that the LES and LE-bo constitute distinct phenotypes of the same functional mutation resulting in severe dysmyelination. Preliminary PCR analysis (data not shown) indicated the same pattern of mutant mRNA isoforms in LE-bo and LES spinal cord extracts,<sup>30</sup> suggesting a common origin of both mutant rat strains in a vendor breeding colony. Subsequent separation of the breeding stock into separate colonies producing dysmyelinated rats (named LES) at McMaster University<sup>12</sup> and the Massachusetts Institute of Technology (LE-bo)<sup>21</sup> apparently resulted in further evolution of either dysmyelinated phenotype with distinct differences in glial cell biology.

The significance of the observation of axonal plasticity in form of sprouting is likely profound. Detailed morphologic examination of the CNS of large numbers of LES and LE-bo rats indicates that axonal sprouting is widespread, occurs throughout the life of both mutant strains, and occurs in direct contact with hypertrophied astrocyte processes or cell membrane of oligodendrocytes or both. Recently published study on long-distance axonal regeneration in the crushed filum terminale,<sup>20</sup> a very small component of the CNS, detected remarkable enhancement of sprouting in the sacral spinal cord in response to nearby injury. Exuberant axonal sprouting was not affected by severe astrogliosis that widely separated individual axons. Therefore, the present and previous<sup>20</sup> study do not support the notion that astrogliosis inhibits axonal

**Figure 7.** Astrogliosis and axonal plasticity in the dysmyelinated rat CNS. (A) Spinal cord, LES rat, 1 wk of age. An area between 2 oligodendrocytes, with unmyelinated axons closely adjacent to each other except for 2 axons with thin, uncompacted sheaths; one of these axons is adjacent to an oligodendrocyte. Bar 2,  $\mu\text{m}$ . (B) Spinal cord, LES rat, 24 wk. Almost all axons in the field adjacent to a hypertrophied astrocyte (As) are separated from each other by astrocytic processes. Bar, 2  $\mu\text{m}$ . (C) Spinal cord, LES rat, 69 wk. Large and medium-sized naked axons (asterisks) are widely separated from each other by astrocytic processes, 1 hypertrophied astrocyte, and 2 immature glial cells, presumably of oligodendroglial lineage. Bar, 4  $\mu\text{m}$ . (D) Optic nerve, LES rat, 16 wk. The cytoplasm of a hypertrophied astrocyte (As) is rich in intermediate filaments (if) and is surrounded by axons, 2 of which have thin uncompacted sheaths, but others are naked and sometimes with microtubules-containing sprouts against the astroglial cell membrane. Bar, 1  $\mu\text{m}$  (inset, 200 nm). (E) Optic nerve, LES rat, 16 wk. One large axon (asterisk) adjacent to an oligodendrocyte (OL) has a thin and incomplete sheath; other axons are unmyelinated, are markedly although not completely separated from each other by astrocytic processes, and often have adjacent clusters of small processes with microtubules (sprouts, circled), sometimes adjacent to the cell membrane of an oligodendrocyte. Bar, 1  $\mu\text{m}$ .

plasticity because astrogliosis does not suppress axonal sprouting. Whether astrogliosis inhibits axonal regeneration in experimental spinal cord injury in dysmyelinated animals remains unknown currently. The long-lived, severely dysmyelinated LE rat strains, especially LES rats, offer unprecedented opportunities to study mechanisms regulating axonal plasticity in the adult CNS.

## Acknowledgments

I thank Dr Kinuko Suzuki for helpful, in-depth introduction to the neuropathology of the dysmyelinating CNS. PCR analysis was performed in the laboratory of Dr S Igdoura (McMaster University). This work was supported by the Dofasco Employee Donations Fund, JP Bickell Foundation, and Multiple Sclerosis Society of Canada.

## References

1. Allen IV, Kirk J. 1992. Demyelinating diseases, p 447–520. In: Adams JH, Duchen LW, editors. Greenfield's neuropathology. New York (NY): Oxford University Press.
2. BaracsKay KL, Duchala CS, Miller RH, Macklin WB, Trapp BD. 2002. Oligodendrogenesis is differentially regulated in gray and white matter of *jimpy* mice. *J Neurosci Res* 70:645–654.
3. Barres BA, Raff MC. 1999. Axonal control of oligodendrocyte development. *J Cell Biol* 147:1123–1128.
4. Baumann N, Pham-Dinh D. 2001. Biology of oligodendrocyte and myelin in the mammalian central nervous system. *Physiol Rev* 81:871–927.
5. Bradl M, Linington C. 1996. Animal models of demyelination. *Brain Pathol* 6:303–311.
6. Bu J, Banki A, Wu Q, Nishiyama A. 2004. Increased NG2<sup>+</sup> glial cell proliferation and oligodendrocyte generation in the hypomyelinating mutant shiverer. *Glia* 48:51–63.
7. Caroni P, Savio T, Schwab ME. 1988. Central nervous system regeneration: oligodendrocytes and myelin as nonpermissive substrates for neurite growth. *Prog Brain Res* 78:363–370.
8. Carroll WM, Jennings AR. 1994. Early recruitment of oligodendrocyte precursors in CNS demyelination. *Brain* 117:563–578.
9. Cerghet M, Bessert DA, Nave K-N, Skoff RP. 2001. Differential expression of apoptotic markers in *jimpy* and in *Plp* overexpressors: evidence for different apoptotic pathways. *J Neurocytol* 30:841–855.
10. Crang AJ, Gilson J, Blakemore WF. 1998. The demonstration of postmitotic oligodendrocytes. *J Neurocytol* 27:541–553.
11. David S, Aguayo AJ. 1981. Axonal elongation into the peripheral nervous system 'bridges' after the central nervous system injury in adult rats. *Science* 214:931–933.
12. Delaney KH, Kwiecien JM, Wegiel J, Wisniewski HM, Percy DH, Fletch AL. 1995. Familial dysmyelination in a Long Evans rat mutant. *Lab Anim Sci* 45:547–553.
13. Dentinger MP, Barron KD, Csiza CK. 1982. Ultrastructure of the central nervous system in a myelin-deficient rat. *J Neurocytol* 11:671–691.
14. Duncan ID, Nadon NL, Hoffman RL, Lunn KF, Csiza C, Wells MR. 1995. Oligodendrocyte survival and function in the long-lived strain of the myelin-deficient rat. *J Neurocytol* 24:745–762.
15. Godfraind C, Friedrich VL, Holmes KV, Dubois-dalcq M. 1989. In vivo analysis of glial cell phenotypes during viral demyelinating disease in mice. *J Cell Biol* 109:2405–2416.
16. Horner PJ, Power AE, Kempermann G, Kuhn HG, Palmer TD, Winkler J, Thal LJ, Gage FH. 2000. Proliferation and differentiation of progenitor cells throughout the intact adult rat spinal cord. *J Neurosci* 20:2218–2228.
17. Inoue Y, Nakamura R, Mikoshiba K, Tsukada Y. 1981. Fine structure of the central myelin sheath in the myelin-deficient mutant *shiverer* mouse, with special reference to the pattern of myelin formation by oligodendroglia. *Brain Res* 219:85–94.
18. Knapp PE, Bartlett WP, Williams LA, Yamada M, Ikenaka K, Skoff RP. 1999. Programmed cell death without fragmentation in the *jimpy* mouse: secreted factors can enhance survival. *Cell Death Differ* 6:136–145.
19. Knapp PE, Skoff RP, Redstone DW. 1986. Oligodendroglial cell death in *jimpy* mice: explanation for the myelin deficit. *J Neurosci* 6:2813–2822.
20. Kwiecien JM, Avram A. 2008. Long-distance axonal regeneration in the filum terminale of adult rats is regulated by ependymal cells. *J Neurotrauma* 25:196–204.
21. Kwiecien JM, Blanco M, Fox JG, Delaney KH, Fletch AL. 2000. Neuropathology of Bouncer Long Evans, a novel dysmyelinated rat. *Comp Med* 50:503–510.
22. Kwiecien JM, O'Connor LT, Goetz BD, Delaney KH, Fletch AL, Duncan ID. 1998. Morphological and morphometric studies of the dysmyelinating mutant, the Long Evans Shaker rat. *J Neurocytol* 27:581–591.
23. Lemke G. 1992. Myelin and myelination, p 281–309. In: Hall ZW, editor. An introduction to molecular neurobiology. Sunderland (MA): Sinauer Associates.
24. Lipsitz D, Goetz BD, Duncan ID. 1998. Apoptotic glial cell death and kinetics in the spinal cord of the myelin-deficient rat. *J Neurosci Res* 51:497–507.
25. Ludwin SK. 1979. An autoradiographic study of cellular proliferation in remyelination of the central nervous system. *Am J Pathol* 95:683–696.
26. Ludwin SK. 1997. The pathobiology of the oligodendrocyte. *J Neuropathol Exp Neurol* 56:111–124.
27. Ludwin SK, Sternberger NH. 1984. An immunohistochemical study of myelin proteins during remyelination in the central nervous system. *Acta Neuropathol* 63:240–248.
28. Lunn KF, Clayton MK, Duncan ID. 1997. The temporal progression of the myelination defect in the *taiep* rat. *J Neurocytol* 26:267–281.
29. Matthieu JM, Roch JM, Omlin FX, Rambaldi I, Almazan G, Braun PE. 1986. Myelin instability and oligodendrocyte metabolism in myelin-deficient mutant mice. *J Cell Biol* 103:2673–2682.
30. O'Connor LT, Goetz BD, Kwiecien JM, Delaney KH, Fletch AL, Duncan ID. 1999. Insertion of a retrotransposon in *Mbp* disrupts mRNA splicing and myelination in a new mutant rat. *J Neurosci* 19:3404–3413.
31. Olfert ED, Cross BM, McWilliam AA, editors. 1993. Guide to the care and use of experimental animals, vol 1. Ottawa (Canada): Canadian Council on Animal Care.
32. Phokeo V, Kwiecien JM, Ball AK. 2002. Characterization of the optic nerve and retinal ganglion cell layer in the dysmyelinated adult Long Evans Shaker rat: evidence for axonal sprouting. *J Comp Neurol* 451:213–224.
33. Popko B, Puckett C, Lai E, Shine HD, Readhead C, Takahashi N, Hunt SW, Sidman RL, Hood L. 1987. Myelin-deficient mice: expression of myelin basic protein and generation of mice with varying levels of myelin. *Cell* 48:713–721.
34. Prineas JW, Barnard RO, Kwon EE, Sharer LR, Cho E-S. 1993. Multiple sclerosis: remyelination of nascent lesions. *Ann Neurol* 33:137–151.
35. Prineas JW, Connell F. 1979. Remyelination in multiple sclerosis. *Ann Neurol* 5:22–31.
36. Prineas JW, Kwon EE, Goldenberg PZ, Ilyas AA, Quarles RH, Benjamins JA, Sprinkle TJ. 1989. Multiple sclerosis, oligodendrocyte proliferation, and differentiation in fresh lesions. *Lab Invest* 61:489–503.
37. Raine CS, Moore GRW, Hintzen R, Traugott U. 1988. Induction of oligodendrocyte proliferation and remyelination after chronic demyelination, relevance to multiple sclerosis. *Lab Invest* 59:467–476.
38. Raine CS, Scheinberg L, Waltz JM. 1981. Multiple sclerosis, oligodendrocyte survival and proliferation in an active established lesion. *Lab Invest* 45:534–546.

39. **Raine CS, Snyder DH, Valsamis MP, Stone SH.** 1974. Chronic experimental encephalomyelitis in inbred guinea pigs, an ultrastructural study. *Lab Invest* **31**:369–380.
40. **Raine CS, Traugott U.** 1983. Chronic relapsing experimental autoimmune encephalomyelitis, ultrastructure of the central nervous system treated with combinations of myelin components. *Lab Invest* **48**:275–284.
41. **Raine CS, Wu E.** 1993. Multiple sclerosis: remyelination in acute lesions. *J Neuropathol Exp Neurol* **52**:199–204.
42. **Readhead C, Popko B, Takahashi N, Shine HD, Saavedra RA, Sidman RL, Hood L.** 1987. Expression of the myelin basic protein gene in transgenic shiverer mice: correction of the dysmyelinating phenotype. *Cell* **48**:703–712.
43. **Rodriguez M, Leibowitz JL.** 1983. Persistent infection of oligodendrocytes in Theiler virus-induced encephalomyelitis. *Ann Neurol* **13**:426–433.
44. **Rodriguez M, Pierce ML, Thiemann RL.** 1991. Immunoglobulins stimulate central nervous system remyelination: electron microscopic and morphometric analysis of proliferating cells. *Lab Invest* **64**:358–370.
45. **Scolding N, Franklin R, Stevens S, Heldin CH, Compston A, Newcombe J.** 1998. Oligodendrocyte progenitors are present in the normal adult human CNS and in lesions of multiple sclerosis. *Brain* **121**:2221–2228.
46. **Skoff RP.** 1982. Increased proliferation of oligodendrocytes in the hypomyelinated mouse mutant *jimpy*. *Brain Res* **248**:19–31.
47. **Skoff RP, Saluja I, Bessert D, Yang X.** 2004. Analyses of proteolipid protein mutants show levels of proteolipid protein regulate oligodendrocyte number and cell death in vitro and in vivo. *Neurochem Res* **29**:2095–2103.
48. **Stryer L.** 1995. Membrane structure and dynamics, p 263–290. In: Stryer L, editor. *Biochemistry*, 4th ed. New York (NY): WH Freeman and Company.
49. **Vela JM, Gonzalez B, Castellano B.** 1998. Understanding glial abnormalities associated with myelin deficiency in the *jimpy* mutant mouse. *Brain Res Brain Res Rev* **26**:29–42.
50. **Watanabe I, Patel V, Goebel HH, Siakotos AM, Zeman W, deMyer W, Dyer JS.** 1973. Early lesions in Pelizaeus–Merzbacher disease: electron microscopic and biochemical study. *J Neuropathol Exp Neurol* **32**:313–333.
51. **Wolswijk G.** 1995. Strongly GD3+ cells in the developing and adult rat cerebellum belong to microglial lineage rather than to oligodendrocyte lineage. *Glia* **13**:13–26.
52. **Wolswijk G.** 2000. Oligodendrocyte survival loss and birth in lesions of chronic-stage multiple sclerosis. *Brain* **123**:105–115.
53. **Wu Q, Miller RH, Ransohoff RM, Robinson S, Bu J, Nishiyama A.** 2000. Elevated levels of the chemokine GRO1 correlate with elevated oligodendrocyte progenitor proliferation in the *jimpy* mutant. *J Neurosci* **20**:2609–2617.
54. **Zhang SC, Goetz BD, Duncan ID.** 2003. Suppression of activated microglia promotes survival and function of transplanted oligodendroglial progenitors. *Glia* **41**:191–198.